Coexistence of weakly and strongly localized donor states in semiconductors

S. Bednarek and J. Adamowski
Faculty of Physics and Nuclear Techniques, Technical University (AGH), Kraków, Poland
(Received 4 December 1995; revised manuscript received 20 September 1996)

A unified theoretical description is proposed for donor states of weak and strong localization. The present approach is based on the one-band approximation and takes into account the couplings with LA and LO phonons. The eigenvalue problem is solved in the wave-vector space by the variational method for several donor states of *s* symmetry. For each excited state, the full orthogonalization is performed, which permits us to include all many-phonon states of lower energy. It is shown that the following two types of donor states can coexist on the same donor impurity: weakly localized hydrogenlike states and strongly localized states. If the energy levels of these distinctly localized donor states become close to each other under influence of some external perturbation, e.g., hydrostatic pressure, then the extremely sharp and narrow anticrossing appears. This effect is due to the very weak level repulsion resulting from the electron-LA phonon coupling. This finding allows us to explain the anomalous anticrossing observed in GaAs. We have shown that the metastability of the excited donor states is caused by the same reason. We have obtained the upper and lower bounds on the probability of radiative transitions from the excited donor state and discussed the conditions for the metastability to appear and to vanish. [S0163-1829(96)08948-5]

I. INTRODUCTION

Donor centers in semiconductors can bind electrons in quantum states of different localization. The potential of the donor center possesses both the long-range (Coulomb) and short-range components. The range of the dominating component of the potential determines the localization of the electron around the donor center. The inverse of the average electron-donor center distance can be treated as a measure of this localization. The two types of donor states with the extreme electron localization play an important role in semiconductors, namely, the states of weak and strong localization. For the weakly localized donor states, the average electron-donor center distance is much larger than the lattice constant, while for the strongly localized donor states, this distance is of the order of the lattice constant. The energy levels of the weakly localized donor states are shallow, i.e., the corresponding energy separations from the conduction band bottom are much smaller than the semiconductor energy gap. In most cases, the energy levels of the strongly localized donor states are deep, i.e., the corresponding energy differences are comparable with (but less than) the energy gap. Usually, the donor states of different localization are observed for different impurity atom species.

This is the conventional picture of the donor states in semiconductors. However, in many semiconductors, both the types of donor states can be formed on the same impurity atom. Such states have been experimentally observed, e.g., in InSb,[1,2] CdF_2,[3,4] GaAs.[5,6] The recent experimental observations in GaAs[6–9] give evidence of the existence of the three different donor states formed on the same impurity atom: (1) weakly localized states with hydrogenlike spectrum, (2) strongly localized state of A_1 symmetry, and (3) the *DX* state. According to the *ab initio* pseudopotential calculations,[10,11] the *DX* state is the highly localized donor center, which is doubly occupied by the electrons and exhibits the negative-*U* behavior and a large lattice deformation. This picture is supported by the experiments.[12–16]

The properties of the neutral donor states of types (1) and (2) are especially interesting if their energy levels are close to each other, i.e., the energy levels of the strongly localized states are shallow. Then, the weakly localized state of slightly higher energy can be metastable with respect to the strongly localized state. The electrons activated from the ground state can occupy the excited weakly localized state for a long time. The metastability has been observed for donors in CdF_2.[3,4] It has been shown in our previous papers[17,18] that the electron-phonon coupling is of crucial importance for understanding this property. This explanation has been supported by the displaced-ion approach.[19]

Other interesting properties of the donor states have been observed in Ge-doped GaAs crystals under hydrostatic pressure.[5,6] At the ambient pressure, the energy level of the strongly localized (A_1) donor state is located at 75 meV above the conduction band bottom. The applied hydrostatic pressure shifts up the minimum of the conduction band together with the energy levels of the weakly localized (hydrogenlike) donor states. The energy level of the strongly localized donor state is weakly dependent on the pressure (its position is determined by the average conduction band). With the increasing hydrostatic pressure, the energy separation between the energy levels associated with both the types of donor states decreases and, at the pressure of about 9 kbar, takes on very small, but nonzero, minimum value. Due to the same symmetry (both the states are *s* type), the corresponding energy levels do not cross but repel each other. The level repulsion for the states of different localization is drastically reduced by the interaction with phonons, which leads to the extremely sharp and narrow anticrossing[20,21] observed as a function of the external pressure and magnetic field.[2,5] In GaAs, the LA phonons play the most important role in this effect.

The problem of coexisting neutral donor states of weak and strong localization requires a special theoretical ap-

proach due to the very subtle effects (in the meV energy regime), which have to be described. The theory should provide a unified description of the states of the weak and strong localization and take into account the quasicontinuous spectrum of many-phonon states, which enters the energy interval between the discrete donor levels. For these states, the *ab initio* approach[11,22] provides only the qualitative results. Most of the existing theoretical methods can be applied to either the weakly or strongly localized donor states. In particular, the effective mass approximation (EMA) leads to the hydrogenlike model of the weakly localized donor states. The simple EMA models for the pressure influence on the hydrogenlike donor states can be found in the papers.[23,24] The correct description of the impurity states with different localization has to go beyond the EMA. In the case of GaAs, it should take into account the conduction-band nonparabolicity.[25,26] The conduction-band structure can be taken on from either the band-structure calculations or an analytical model. Such model approach to magnetopolaron effects in GaAs was proposed by Shi *et al.*[27]

In the first theoretical papers,[28–30] the coordinate-space representation and EMA were applied to the impurity states of the different electron localization. The long-range and short-range components of the impurity potential were included. Toyozawa[31] additionally included the coupling with phonons in the frame of the continuous deformable-lattice model, which yielded a qualitative description of the coexisting donor states. We proposed an another approach,[17,18,32,33] which is based on the wave-vector space representation for both the electron and phonon states in the Brillouin zone. Instead of the EMA, we apply the more general one-band approximation. The first paper of our work has been recently published.[21] The present paper provides the full presentation of our method, the complete results, and detailed discussion. Section II contains the presentation of the method, applied approximations, and results for the energy levels and localization of the donor states in GaAs. In Sec. III, we consider the probability of radiative transitions from the excited donor state. The discussion and interpretation of the results is given in Secs. IV and V. Special attention is paid to the description of anomalous anticrossing and metastability of donors. In the Appendix, we present the method of obtaining the estimates for the transition probability considered in Sec. III.

II. EIGENVALUE PROBLEM FOR ELECTRON-DONOR-PHONON SYSTEM

We consider the system composed of the electron, the donor center and the deformable crystal lattice. The lattice deformations are described in terms of phonon fields. The Hamiltonian of the system has the following form:

$$H = H_0 + H_1 + H_2 + H_3, \tag{1}$$

where H_0 describes the noninteracting conduction-band electrons and phonons, H_1 the electron-donor center interaction, H_2 the electron-phonon interaction, and H_3 the donor-phonon interaction. In the present work, we apply the occupation number representation for both the electrons and phonons and assume the one-band approximation for the electron-donor subsystem. The Hamiltonian H_0 takes on the form

$$H_0 = \sum_{\mathbf{k}} E^c_{\mathbf{k}} b^\dagger_{\mathbf{k}} b_{\mathbf{k}} + \sum_{\sigma\mathbf{q}} \hbar\omega_{\sigma\mathbf{q}} a^\dagger_{\sigma\mathbf{q}} a_{\sigma\mathbf{q}}, \tag{2}$$

where $E^c_{\mathbf{k}}$ is the conduction-band energy, $b^\dagger_{\mathbf{k}}$ ($b_{\mathbf{k}}$) is the creation (annihilation) operator of the Bloch state of the conduction-band electron, $a^\dagger_{\sigma\mathbf{q}}$ ($a_{\sigma\mathbf{q}}$) is the creation (annihilation) operator of the phonon state with the energy $\hbar\omega_{\sigma\mathbf{q}}$, wave vector $\mathbf{q}$, and branch index σ. We take into account the longitudinal acoustic (LA) and longitudinal optical (LO) phonons, i.e., $\sigma = \mathrm{LA, LO}$. The Hamiltonian of electron-donor center interaction has the form

$$H_1 = \sum_{\mathbf{k}\mathbf{k}'} V_{\mathbf{k}\mathbf{k}'} b^\dagger_{\mathbf{k}} b_{\mathbf{k}'}, \tag{3}$$

where $V_{\mathbf{k}\mathbf{k}'} = V^C_{\mathbf{k}-\mathbf{k}'} + V^S_{\mathbf{k}\mathbf{k}'}$ is the potential-energy matrix element between the two Bloch states. The potential energy of the electron in the donor-center field is the sum of the long-range (V^C) and short-range (V^S) components. We take on the long-range component in the Coulomb form screened by the high-frequency dielectric constant ε_∞.

In the most general case, the electron-phonon interaction Hamiltonian can be written as

$$H_2 = \sum_{\sigma\mathbf{k}\mathbf{q}} F_{\sigma\mathbf{k}\mathbf{q}} (a_{\sigma\mathbf{q}} b^\dagger_{\mathbf{k}+\mathbf{q}} b_{\mathbf{k}} + \mathrm{H.c.}) \tag{4}$$

and the interaction Hamiltonian of the donor center with phonons as

$$H_3 = \sum_{\sigma\mathbf{q}} (W_{\sigma\mathbf{q}} a_{\sigma\mathbf{q}} + \mathrm{H.c.}), \tag{5}$$

where $F_{\sigma\mathbf{k}\mathbf{q}}$ and $W_{\sigma\mathbf{q}}$ are the electron-phonon and donor-phonon interaction amplitudes, respectively. We assume that the electron-phonon interaction amplitudes are independent of the electron wave vector $\mathbf{k}$, i.e., $F_{\sigma\mathbf{k}\mathbf{q}} = F_{\sigma\mathbf{q}}$.

Hamiltonian (1) provides an example of a general problem of a fermion system interacting with two boson fields. Specifying the forms of the interaction amplitudes and dispersion relations, we will be able to apply Hamiltonian (1) to the problem of donor in a semiconductor.

In the present approach, we first transform Hamiltonian (1) using the canonical transformation introduced by Platzman[34]

$$U_P = \exp\left\{ \sum_{\sigma\mathbf{q}} [(W_{\sigma\mathbf{q}}/\hbar\omega_{\sigma\mathbf{q}}) a_{\sigma\mathbf{q}} - \mathrm{H.c.}] \right\}, \tag{6}$$

which yields the transformed Hamiltonian $\overline{H} = U^\dagger_P H U_P$ in the form

$$\overline{H} = H_0 + H_2 + \sum_{\mathbf{k}\mathbf{k}'} \overline{V_{\mathbf{k}\mathbf{k}'}} b^\dagger_{\mathbf{k}} b_{\mathbf{k}'} - \sum_{\sigma\mathbf{q}} |W_{\sigma\mathbf{q}}|^2/\hbar\omega_{\sigma\mathbf{q}}. \tag{7}$$

The matrix elements in the third term take on the form

$$\overline{V_{\mathbf{k}\mathbf{k}'}} = \overline{V^C_{\mathbf{k}-\mathbf{k}'}} + \overline{V^S_{\mathbf{k}\mathbf{k}'}}, \tag{8}$$

where

$$\overline{V^C_{\mathbf{k}-\mathbf{k}'}} = V^C_{\mathbf{k}-\mathbf{k}'} - (F_{LO,\mathbf{k}-\mathbf{k}'} W^*_{LO,\mathbf{k}-\mathbf{k}'}/\hbar\omega_{LO,\mathbf{k}-\mathbf{k}'} + \text{c.c.}) \tag{9}$$

and

$$\overline{V^S_{\mathbf{k}\mathbf{k}'}} = V^S_{\mathbf{k}\mathbf{k}'} - (F_{LA,\mathbf{k}-\mathbf{k}'} W^*_{LA,\mathbf{k}-\mathbf{k}'}/\hbar\omega_{LA,\mathbf{k}-\mathbf{k}'} + \text{c.c.}). \tag{10}$$

In Eqs. (9) and (10), we have included the mixed terms, which consist of the electron-phonon and donor-phonon interaction amplitudes, into the matrix elements of the potential energy of the electron in the donor-center field. Both the terms in Eq. (9) correspond to the long-range potentials. If we take on the Fröhlich coupling with LO phonons [cf. Eq. (26)], then $\overline{V^C}$ becomes the potential energy of the electron in the Coulomb field screened by the static dielectric constant ε_0. The second term in Eq. (10) results from the short-range electron-LA phonon interaction. In the following, we assume the short-range interaction (10) to be local, i.e., $\overline{V^S_{\mathbf{k}\mathbf{k}'}} = \overline{V^S_{\mathbf{k}-\mathbf{k}'}}$. The last term in Eq. (7) possesses the meaning of the self-energy, which corresponds to the energy of the lattice deformation around the donor center.

Before going further, let us briefly discuss the physical interpretation of the result of Platzman transformation (6). This transformation introduces the self-energy of the donor center and modifies the electron-donor center interaction due to the screening of the long-range (Coulomb) interaction and adding the short-range interaction caused by the exchange of virtual LA phonons. These terms in transformed Hamiltonian (7) yield the largest contribution to the energy, which originates from the phonon field. In the conventional approach[34,35] to the bound polaron problem, the self-energy term is infinite. In the present approach, this term is finite and determines the lattice relaxation energy around the donor center. For example, we have estimated[17,18] this energy for CdF_2 to be 1.6 eV in agreement with experiment.[4] The constant self-energy shifts the energy levels of all the donor states by the same value. Since in the present work we are interested in the energy differences between the donor levels, we omit this term in the further considerations.

In order to solve the eigenvalue problem for Hamiltonian (7), we apply the variational method with the following expansion of the eigenvector in the many-element basis:

$$|\Psi\rangle = \sum_i c_i |\psi_i\rangle, \tag{11}$$

where c_i are the linear variational parameters. For the first three states of s symmetry, the satisfactory results are obtained with the use of the ten-element basis. Each basis state in Eq. (11) is taken to be the product of the electron and phonon states, i.e.,

$$|\psi_i\rangle = |\Phi_i\rangle|\chi_i\rangle. \tag{12}$$

The electronic state has the form

$$|\Phi_i\rangle = \sum_{\mathbf{k}} \phi_{i\mathbf{k}} b^\dagger_{\mathbf{k}} |0\rangle_{el}, \tag{13}$$

where $|0\rangle_{el}$ is the electron vacuum state. We propose the variational form of the functions

$$\phi_{i\mathbf{k}} = N_i (1 + k^2/\alpha_i^2)^{-2}, \tag{14}$$

where α_i are the nonlinear variational parameters and N_i are the normalization constants, which assure the normalization of functions (14) in the first Brillouin zone. We introduce the electron density for the ith basis state

$$\rho_{i\mathbf{q}} = \sum_{\mathbf{k}} \phi^*_{i,\mathbf{k}+\mathbf{q}} \phi_{i\mathbf{k}}, \tag{15}$$

which possesses the following properties:

$$\rho_{i\mathbf{q}} = \rho_{i,-\mathbf{q}} = \rho^*_{i\mathbf{q}}. \tag{16}$$

The phonon state in Eq. (12) has the form

$$|\chi_i\rangle = U_i |0\rangle_{ph}, \tag{17}$$

where $|0\rangle_{ph}$ is the phonon vacuum state. The operator of the unitary transformation in Eq. (17) is proposed in the form

$$U_i = \exp\left(\sum_{\sigma\mathbf{q}} g_{i\sigma\mathbf{q}} a^\dagger_{\sigma\mathbf{q}} - \text{H.c.} \right), \tag{18}$$

where the phonon amplitudes have been chosen as

$$g_{i\sigma\mathbf{q}} = -F^*_{\sigma\mathbf{q}} \rho_{i\mathbf{q}}/\hbar\omega_{\sigma\mathbf{q}}. \tag{19}$$

The overlap between two phonon states (17)

$$S_{ij} = \langle\chi_i|\chi_j\rangle = \exp\left[-\frac{1}{2} \sum_{\sigma\mathbf{q}} |F_{\sigma\mathbf{q}}|^2 |\rho_{i\mathbf{q}} - \rho_{j\mathbf{q}}|^2/(\hbar\omega_{\sigma\mathbf{q}})^2 \right] \tag{20}$$

is an important auxiliary quantity in the present treatment. The overlap-matrix elements between basis states (12) are given by

$$P_{ij} = \sum_{\mathbf{k}} \phi^*_{i\mathbf{k}} \phi_{j\mathbf{k}} S_{ij} \tag{21}$$

and the matrix elements of Hamiltonian (7) by

$$H_{ij} = S_{ij} \sum_{\mathbf{k}} \left[E^c_{\mathbf{k}} \phi^*_{i\mathbf{k}} \phi_{j\mathbf{k}} + \sum_{\mathbf{k}'} \overline{V_{\mathbf{k}-\mathbf{k}'}} \phi^*_{i\mathbf{k}} \phi_{j\mathbf{k}'} - \sum_{\sigma\mathbf{q}} |F_{\sigma\mathbf{q}}|^2 (\rho_{i\mathbf{q}} + \rho_{j\mathbf{q}}) \phi^*_{i\mathbf{k}+\mathbf{q}} \phi_{j\mathbf{q}}/\hbar\omega_{\sigma\mathbf{q}} \right] + P_{ij} \sum_{\sigma\mathbf{q}} |F_{\sigma\mathbf{q}}|^2 \rho_{i\mathbf{q}} \rho_{j\mathbf{q}}/\hbar\omega_{\sigma\mathbf{q}}. \tag{22}$$

Using matrix elements (21) and (22), we solve the eigenvalue problem for the nonorthogonal basis

$$\sum_j H_{ij} C_{jn} = E_n \sum_j P_{ij} C_{jn}. \tag{23}$$

The minimization of E_n over the nonlinear parameters is performed for each n, separately. The variational calculation with the many-element basis is equivalent to the method of outer projection[36] on the subspace spanned by these basis states. Therefore, the minimization of the excited-state energy leads to a change of the projection operator. As a result, the corresponding trial wave function is not orthogonal to the

optimized wave functions for the states of lower energy but is orthogonal to the wave functions providing the upper bounds, which are not the best variational estimates, nevertheless, they are lying below the considered energy level. The variational estimates obtained by this method provide a set of correct upper bounds[36] to the true energy eigenvalues (cf. Appendix of Ref. 35).

If the short-range potential is repulsive or weakly attractive, the effective-mass approximation (EMA) can be applied. In this case, the band energy together with the Coulomb potential energy lead to the hydrogenlike donor spectrum, provided that the conduction band minimum is at $\mathbf{k}=0$. If we moreover take into account the electron-phonon coupling, we obtain the classical problem of the bound polaron.[35]

If the short-range potential is attractive and sufficiently strong, the highly localized donor state can be created. The wave function of such state is spread out over the entire Brillouin zone; therefore, the effective-mass approximation is no more applicable. In order to describe these states we have to know the conduction band dispersion relation and the electron-phonon interaction amplitudes in the entire Brillouin zone. For the present purpose, we cannot use the methods applicable for the deep-level impurity states, since the considered donor states possess the shallow energy levels (lying in the interval of a few meV below the conduction band). Instead, we apply the one-band approximation, which allows us to describe the weakly and strongly localized donor states within the same unified approach.[33] The present method is based on the assumption that the shallow-level donor states of arbitrary localization are formed from the states of the lowest conduction band, which possesses the average width Δ and the minimum in the center of the Brillouin zone, and is characterized by the effective band mass m_e at the Γ point. The dispersion relation for the conduction band is proposed in the analytical form[33]

$$E_{\mathbf{k}}^{c}=\frac{t_{\mathbf{k}}}{1+t_{\mathbf{k}}/\Delta}, \tag{24}$$

where $t_{\mathbf{k}}=\hbar^2k^2/2m_e$ is the conduction-band form in the EMA. For small $|\mathbf{k}|$, $E_{\mathbf{k}}^{c}\rightarrow t_{\mathbf{k}}$; therefore, our approach goes over into the EMA.

For GaAs, we take on the following values of the parameters: $\Delta=1.1$ eV and $m_e=0.0656m_{e0}$, where m_{e0} is the electron rest mass. The applicability of formula (24) to the lowest conduction band relies on the following arguments: First, we have performed the empirical-pseudopotential calculations, the results of which are plotted in Fig. 1 and compared with those of Eq. (24). We see that formula (24) provides the average conduction band for GaAs, where the averaging is performed over the entire Brillouin zone. Second, in Fig. 2. we have shown the several analytical forms for the lowest conduction band of GaAs near the center of the Brillouin zone. In particular, we see that in the energy interval [0, 0.6 eV] above the conduction band bottom, the present analytical formula reproduces the fitted form,[25] which takes into account the nonparabolicity of the conduction band in GaAs. If $|\mathbf{k}|$ increases, function (24) asymptotically tends to its value at the Brillouin zone boundary. On the contrary, the form[25] becomes unphysical (see Fig. 2, which also shows the results

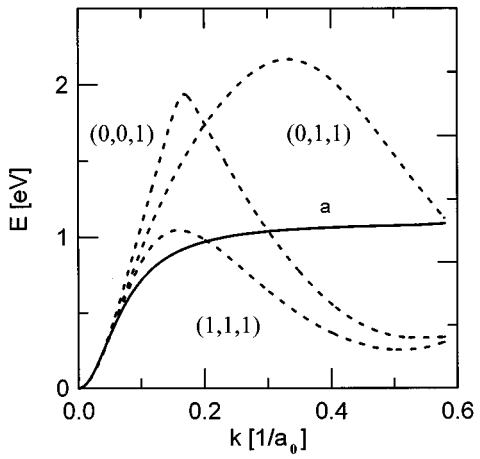

FIG. 1. The lowest conduction band in GaAs as a function of the wave vector **k**. Dashed curves show the results of the empirical-pseudopotential calculations for the directions (1,1,1), (0,0,1), and (0,1,1), solid curve (a) corresponds to the analytical form [Eq. (24)]. a_0 is the hydrogen Bohr radius.

of Ruf and Cardona[26] and the parabolic approximation $t_{\mathbf{k}}$). The conduction band in GaAs possesses the global minimum at the Γ point and the subsidiary minima at the L and X points (Fig. 1). Since these subsidiary minima are located considerably higher than the Γ minimum, they do not affect the shallow-level donor states connected with the Γ point; therefore, we neglect them in the present treatment.

In the present calculations, all the summations over the Brillouin zone in Eqs. (21) and (22) are replaced by the integrations over the Debye sphere of the same volume. For GaAs, the radius of the Debye sphere is taken on to be $Q=0.57a_0^{-1}$, where a_0 is the hydrogen-atom Bohr radius. The double sums over the first Brillouin zone in Eq. (22) are evaluated by the integration over the two independent Debye spheres. When calculating the third term in Eq. (22), we have

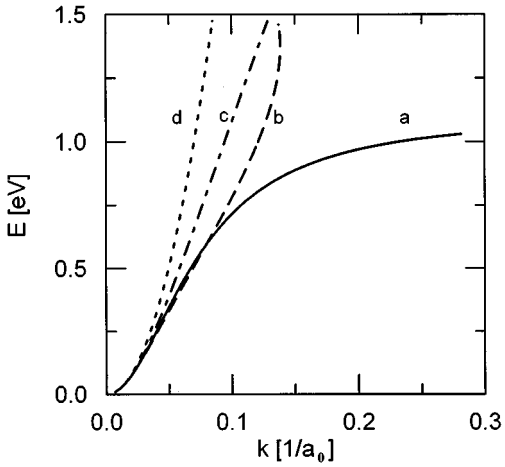

FIG. 2. Comparison of several analytical forms for the lowest conduction band in GaAs near the center of the Brillouin zone. Curve (a) corresponds to the present analytical form [Eq. (24)], (b) to the form fitted by Ekenberg [Ref. 25], (c) to the form of Ruf and Cardona [Ref. 26], and (d) to the effective-mass approximation with the electron band mass $m_e=0.0656m_{e0}$.

to proceed with a special caution and take into account the fact that the three vectors, namely, **k**, **q**, and **k+q** lie within the first Brillouin zone.

The short-range potential is taken to be a constant in the wave-vector space, i.e., $\overline{V_{\mathbf{k}}^{S}}=\gamma$ if $|\mathbf{k}|\leqslant Q$, which corresponds to the Fourier transform of the Dirac δ-like potential in the configurational space. The parameter γ may be determined from the difference of the atomic core potentials of the impurity and the host crystal atoms. In the present approach, however, we treat γ as a fitting parameter.

In the description of the electron-phonon interaction, we assume the deformation potential coupling with LA phonons and the polar Fröhlich coupling with LO phonons. The interaction amplitude for LA phonons has the form

$$F_{LA,\mathbf{q}}=D\left(\frac{\hbar}{2c\rho\Omega}\right)^{1/2}q^{1/2}, \tag{25}$$

where D is the deformation-potential constant, c is the velocity of sound, ρ is the mass density of the crystal, and Ω is the quantization volume. The dispersion relation for the LA phonons is assumed to be isotropic and linear as a function of the wave-vector length, i.e., $\hbar\omega_{LA,\mathbf{q}}=(q/Q)\hbar\omega_{LO}$. The applicability of interaction amplitude (25) is limited to the small q region, which is sufficient for the discussed properties. In GaAs, the polar coupling with LO phonons is weak; however, it shifts the shallow energy levels by several percent, and has to be included in order to bring the calculated values into agreement with experiment. The corresponding interaction amplitude is taken on in the Fröhlich form

$$F_{LO,\mathbf{q}}=-i\left[\frac{2\pi e^2\hbar\omega_{LO}}{\Omega}\left(\frac{1}{\varepsilon_\infty}-\frac{1}{\varepsilon_0}\right)\right]^{1/2}\frac{1}{q}. \tag{26}$$

The amplitude of the donor-LO phonon interaction is given by $W_{LO,\mathbf{q}}=-F_{LO,\mathbf{q}}$, while that for LA phonons enters only the constant terms: self-energy in Eq. (7) and short-range potential [Eq. (10)]. Thus, its q dependence plays no role in the present approach.

The variational procedure for the excited states requires the orthogonalization of the considered mth state to the states (labeled by n), which possess the lower energies, i.e., $E_n<E_m$ for $n<m$. The phonon field introduces additional states to the system. If we take into account the dispersionless LO phonons, we need no special treatment, since the LO phonon energy (for GaAs: 36 meV) is greater than the separations between the considered energy levels ($\sim$6 meV). A new problem arises if we include the LA phonons. Then, below the mth excited-state energy level, there exists a band of many-phonon energy levels corresponding to the following excited states of the system: the donor in the ground state plus many created phonons. The considered mth state has to be orthogonal to all these many-phonon states. In order to perform this orthogonalization, we proceed as follows: First, we define after Löwdin[36] the operator O_m of the outer projection onto the states orthogonal to those involving the phonons with the energy $\hbar\omega_{LA,\mathbf{q}}<E_m-E_0$, where E_0 is the ground-state energy. This projection operator allows us to construct the new phonon states

$$|\overline{\chi}\rangle=O_m^{\dagger}|\chi\rangle, \tag{27}$$

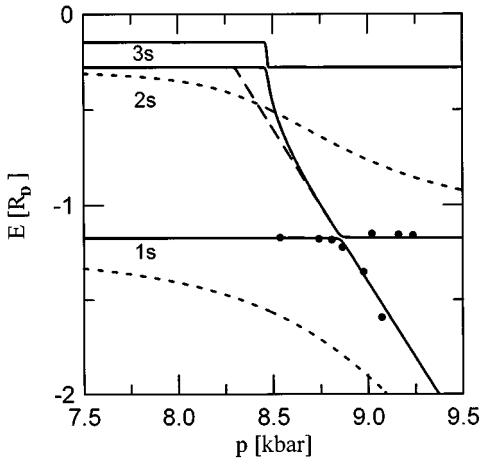

FIG. 3. Calculated donor energy levels in GaAs as functions of hydrostatic pressure. Solid curves show the results obtained when both the LO and LA phonons are taken into account and the full orthogonalization is performed according to Eq. (28); dashed curve, those when projection (28) is omitted, and dotted curves, those when only the LO phonons are included. Dots correspond to the experimental points. The parameter of the short-range potential $\gamma=-0.168$ eV for the solid curves and $\gamma=-0.336$ eV for the dotted curves. Energy is measured with respect to the conduction-band minimum in donor Rydbergs (R_D).

and the projected Hamiltonian[36]

$$\bar{\bar{H}}=O_m^{\dagger}\overline{H}O_m. \tag{28}$$

Projection (27) eliminates from the calculations the subspace of many-phonon states, which corresponds to the phonons of the energy: $0\leqslant\hbar\omega_{LA,\mathbf{q}}<E_m-E_0$. The same operator ensures the orthogonality of the considered mth state to all excited many-phonon states of lower energy, because their eigenvalues E_n are located at the energy separation smaller than that for the ground state. In this case, the condition $\hbar\omega_{LA,\mathbf{q}}<E_m-E_n$ is automatically fulfilled. The ground-state energy is calculated with the use of the full Hamiltonian H; however, the calculations for the mth excited state are performed with the use of the projected Hamiltonian $\bar{\bar{H}}$, which guarantees the orthogonality of all the considered states.

This procedure has been applied to the donor states in GaAs under the hydrostatic pressure. The influence of the hydrostatic pressure has been taken into account by introducing the pressure dependence of the material parameters known from experiment. The electron-band mass and the static dielectric constant depend on the pressure p as follows:[5] $m_e(p)=m_e(0)(1+6.15\times10^{-3}p-1.22\times10^{-5}p^2)$ and $\varepsilon_0(p)=\varepsilon_0(0)\exp(-1.73\times10^{-3}p)$, where p is expressed in kbars. The donor energy levels are determined with respect to the bottom of the conduction band. Therefore, when introducing the pressure dependence of the average conduction-band width Δ in Eq. (24), we take into account the relative shift of the conduction-band minimum with respect to the average conduction band. The pressure coefficient of the parameter Δ is estimated by the similar way as that of Ref. 10 and takes on the value $d\Delta/dp=-0.0087$ eV/kbar.

The calculated energy levels for the donor states of s symmetry are shown in Fig. 3 as functions of the hydrostatic pressure. The experimental data are also shown for comparison. One can notice that the position of zero on the energy scale corresponds to the conduction-band minimum, which moves with pressure when determined with respect to the valence-band maximum. The results obtained with the help of projection (28) with both the LA and LO phonons included are shown by solid curves; the dashed curve shows the estimate of the first excited-state energy, which is obtained if projection (28) is not performed. The solid curves provide the correct variational upper bounds on the energy levels, while the dashed curve can be regarded as the corresponding lower bound. The solid curves in Fig. 3 agree very well with the observed behavior of the donor energy levels in GaAs under hydrostatic pressure. Their characteristic shape is due to the anticrossing between the energy level associated with the strongly localized donor state and the hydrogenlike energy levels of the weakly localized donor states. If we increase the applied pressure, first the higher energy levels fall down and can closely approach the ground-state energy level before this level starts to drop off. The relative change (with respect to the conduction-band bottom) of the energy level of the strongly localized state is very rapid and can be traced in Fig. 3 with the help of the curve, which interpolates between the steeply descending parts of solid curves. The energy level associated with the strongly localized state enters the energy gap at 8.5 kbar and subsequently modifies the hydrogenlike energy levels; first those of the highest energy associated with the excited states and next that of the ground state.

The deformation-potential interaction with LA phonons is of a crucial importance in this behavior. In order to determine the role of this interaction, we have shown in Fig. 3 the energy levels calculated with neglected LA phonons (dotted curves). The omission of the short-range interaction mediated by the virtual LA phonons shifts the anticrossing toward high pressures ($\sim$ 25 kbar).[20] In the present paper, we have changed the value of the electronic short-range potential γ, which is the fitting parameter in the present approach, and shifted back the anticrossing obtained without the LA phonons to the experimentally measured pressure regime. The curves obtained with and without the LA phonons exhibit a remarkable qualitative difference. If we neglect the interaction with LA phonons, the $1s$ and $2s$ energy levels gradually fall down with increasing pressure. Their anticrossing with the energy level of the highly localized state is characteristic of a strong repulsion between the energy levels. The electronic wave functions consist of the strongly and weakly localized basis elements, which are mixed in a relatively broad pressure regime. If we incorporate the interaction with LA phonons, the overlap between the phonon parts of the wave functions for the strongly and weakly localized states is considerably reduced. The electronic wave functions of strong and weak localization are mixed only in the closest vicinity of anticrossing. As a result, the level repulsion becomes very weak, which is responsible for the very sharp and narrow anticrossing.

The anomalous properties of the donor states are closely connected with their localization. In order to point out this relation, we have calculated the expectation values of the electron-donor center distance for the considered states (Fig. 4). The localization of the corresponding states can be regarded as to be inversely proportional to this distance. The calculated average electron-donor separations indicate how large is the mixing of distinctly localized basis states (12). Outside the regions of anticrossing, the donor states are weakly localized and their average radii are close to those of the hydrogenlike donor states, i.e., donor Bohr radii. If the pressure approaches the values, at which the energy levels in Fig. 3 exhibit the anticrossing, the average donor radii are very rapidly changed, i.e., the localization of electron around the donor center is respectively changed. The horizontal line beginning at about 8.5 kbar corresponds to the strongly localized state, for which the average electron-donor distance takes on the constant value $0.0185 a_D$.

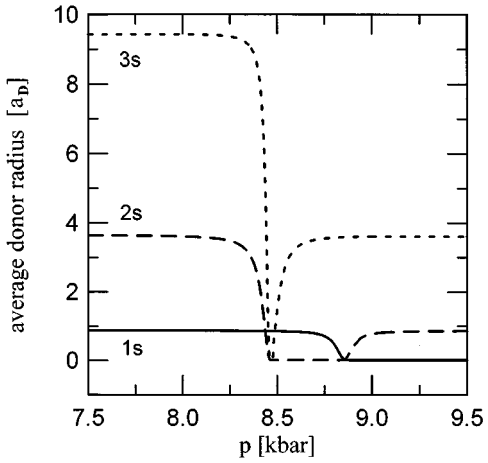

FIG. 4. Expectation values of the electron-donor center distance calculated as functions of hydrostatic pressure for several donor states. The unit of length is the donor Bohr radius a_D.

III. PROBABILITY OF OPTICAL TRANSITIONS

Let us consider now the influence of the interaction with phonons on the optical transitions between the donor states. We will show that the electron-phonon coupling essentially changes the probability of radiative transitions between the donor states of different electron localization. This effect results from the difference of lattice deformation for both the types of donor states and can lead to the metastability of the excited states.

According to the results of Sec. II, the donor wave functions are constructed as linear combinations of the basis functions of weak and strong localization. It appears, however, that only in the anticrossing regime the basis functions of different localization are strongly mixed with each other. This can be seen from Fig. 4, which shows that the donor radii take on the intermediate values (between those corresponding to either the weak or strong localization) only in the very narrow intervals of pressure near the anticrossing. If the pressure exceeds the values from this narrow anticrossing regime, the ground-state donor radius rapidly decreases, reaching the small value characteristic for the highly localized state, while the excited-state donor radius immediately approaches the value corresponding to the previous weakly localized state. Therefore, the ground state becomes highly

localized, while the excited states remain weakly localized. For these states of different localization, one can expect the metastability to occur. Based on the results of Sec. II, we approximate the ground-state wave function by the single, strongly localized basis function (12). On the other hand, the excited-state wave function is approximated by the single, weakly localized basis function. We are interested in the probability of leaving the initial state (weakly localized $2p$ donor state) and reaching one of the final states (strongly localized donor states of s symmetry) in one-electron transitions. At low temperatures, these transitions can only be caused by an external perturbation, which is the electron-photon interaction. Thus, we consider the spontaneous radiative transitions from the initial state with energy E_1

$$|\Psi_1\rangle = |\Phi_1\rangle|\chi_1\rangle \tag{29}$$

to the final states with energies E_f

$$|\Psi_f\rangle = |\Phi_f\rangle|\chi_f\rangle. \tag{30}$$

The set of the final states consists of all the states with energies lower than E_1, i.e., the highly localized ground state $|\Psi_0\rangle = |\Phi_0\rangle|\chi_0\rangle$ as well as the states $|\Psi_f\rangle = |\Phi_0\rangle|\chi_{0N}\rangle$, in which the electron-donor subsystem is in the state $|\Phi_0\rangle$ and there exist the many-phonon states of the form

$$|\chi_{0N}\rangle = U_0 \prod_{\sigma} \frac{1}{\sqrt{N_\sigma!}} \prod_{j=1}^{N_\sigma} a^{\dagger}_{\sigma \mathbf{q}_{\sigma j}} |0\rangle_{ph}. \tag{31}$$

Here, N_{LA} and N_{LO} are the numbers of LA and LO phonons, respectively, $N = N_{LA} + N_{LO}$ is the total number of phonons, and the operator U_0 is given by Eq. (18).

The probability of the spontaneous radiative transitions from the initial state $|\Psi_1\rangle$ to the final states $|\Psi_f\rangle$ of the discrete spectrum with the emission of the photon with the energy $E_1 - E_f$ can be written in the form

$$P = \sum_f \left| \langle \Psi_1 | \sum_{\mathbf{k}\mathbf{k}'} w_{\mathbf{k}\mathbf{k}'} b^{\dagger}_{\mathbf{k}} b_{\mathbf{k}'} | \Psi_f \rangle \right|^2 (E_1 - E_f), \tag{32}$$

where, in the dipole approximation, the electron-photon matrix element is given by

$$w_{\mathbf{k}\mathbf{k}'} = A \langle \psi^c_{\mathbf{k}} | \nabla \cdot \boldsymbol{\varepsilon} | \psi^c_{\mathbf{k}'} \rangle. \tag{33}$$

Here, A is the constant dependent on the material parameters, but independent of the photon energy, $\boldsymbol{\varepsilon}$ is the photon polarization vector, and $\psi^c_{\mathbf{k}}$ is the Bloch wave function of the conduction band.

After substituting into Eq. (32) the expressions for the initial and final states, we get the total transition probability in the form of the product

$$P = P_{el} P_{ph}, \tag{34}$$

of the electronic part

$$P_{el} = \Delta E \left| \sum_{\mathbf{k}\mathbf{k}'} \phi^*_{1\mathbf{k}} w_{\mathbf{k}\mathbf{k}'} \phi_{0\mathbf{k}'} \right|^2 \tag{35}$$

and the phonon part

$$P_{ph} = (\Delta E)^{-1} \sum_{\{N\}} |\langle \chi_1 | \chi_{0N} \rangle|^2 \Delta E_N \Theta(\Delta E_N), \tag{36}$$

where

$$\Delta E = E_1 - E_0 \tag{37}$$

and

$$\Delta E_N = \Delta E - \sum_{\sigma} \sum_{j=1}^{N_\sigma} \hbar \omega_{\sigma \mathbf{q}_{\sigma j}}. \tag{38}$$

In Eq. (36), Θ is the step function, which is equal to 1 for the positive value of argument and 0 for the negative one. The sum over $\{N\}$ in Eq. (36) is a shorthand for the summation over all the states of LA and LO phonons in the Brillouin zone, i.e., the summation over all the possible combinations of numbers of the created phonons, and their wave vectors. In particular, this means that in Eq. (36) we deal with the manyfold summation over the Brillouin zone (cf. the Appendix). The overlap between the phonon states in Eq. (36) is calculated to be [cf. Eq. (20)]

$$\langle \chi_1 | \chi_{0N} \rangle = S_{10} \prod_{\sigma} \frac{1}{\sqrt{N_\sigma!}} \prod_{j=1}^{N_\sigma} (g_{1\sigma \mathbf{q}_{\sigma j}} - g_{0\sigma \mathbf{q}_{\sigma j}})^*. \tag{39}$$

Inserting Eq. (39) into Eq. (36), we obtain

$$P_{ph} = (\Delta E)^{-1} |S_{10}|^2 \sum_{\{N\}} \prod_{\sigma} \frac{1}{N_\sigma!} \prod_{j=1}^{N_\sigma} |g_{1\sigma \mathbf{q}_{\sigma j}} - g_{0\sigma \mathbf{q}_{\sigma j}}|^2 \times \Delta E_N \Theta(\Delta E_N). \tag{40}$$

If we consider only the LO phonons (with constant nonzero energies), then, because of the Θ function, we have the finite number of many-phonon states with energies belonging to the interval (E_0, E_1). The number N_{LO} takes on the values from 0 to N_{LO}^{max} which is determined by the condition

$$\Delta E - N_{LO}^{max} \hbar \omega_{LO} \geqslant 0. \tag{41}$$

In this case, we can calculate P_{ph} exactly. If we include the LA phonons, an arbitrary large number of low-energy LA phonons can appear in the energy interval (E_0, E_1). Then, the sum over $\{N\}$ in Eq. (40) becomes infinite with the infinite-fold summation over the phonon wave vectors. The exact evaluation of this sum is impossible. Nevertheless, we have succeeded (see the Appendix) in calculating the lower (P_L) and upper (P_U) bounds on the probability P_{ph}, i.e.,

$$P_L \leqslant P_{ph} \leqslant P_U. \tag{42}$$

Figure 5 shows the estimated phonon factor P_{ph} of the probability of radiative transitions from the excited $2p$ state to all states with lower energies, i.e., ground state plus N-phonon states. The lower and upper bounds on P_{ph} are plotted as functions of the energy-level separation $\Delta E = E_1 - E_0$. The two solid curves show these bounds for GaAs and the two dashed curves, for CdF_2. The calculated lower and upper bounds lie close to each other in a large part of the transition energy interval. The results of the exact calculation of the transition probability P_{ph} for the LO phonons are shown by the dotted curve, which exhibits the

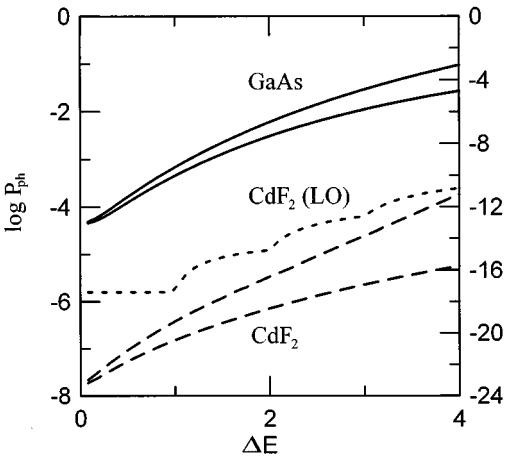

FIG. 5. Phonon factor P_{ph} of the probability of radiative transitions from the excited $(2p)$ donor state to lower-lying states as a function of the energy separation $\Delta E = E_1 - E_0$ between the $2p$ state and ground state. The two upper solid curves show the upper and lower bound on P_{ph} for GaAs, the two lower dashed curves show those for CdF_2. The dotted curve shows the results of the exact calculation for CdF_2 with only LO phonons taken into account. The left scale corresponds to GaAs and CdF_2 (LO), the right scale to CdF_2 with both the LO and LA phonons included. The unit of energy is the LO-phonon energy, log is the logarithm to the base 10.

characteristic steps if the transition energy is equal to the multiplicity of the LO phonon energy.

IV. DISCUSSION

Let us discuss the results of Secs. II and III shown in Figs. 3–5. Figure 3 shows the energy levels of the donor states of *s* symmetry in GaAs as functions of the hydrostatic pressure. In the considerable intervals of pressure, the energy levels corresponding to the weakly localized donor states form the slightly distorted hydrogenlike spectrum. These energy levels do not change with respect to the conduction-band bottom, which is a characteristic property of the states of weak localization. The properties of the strongly localized donor state are different. This state is resonant with the conduction band for the pressures below 8.5 kbar. The corresponding energy level enters the energy gap at higher pressure, which changes the energy spectrum in a narrow interval of pressure. In this discussion, we use the hydrogenic labels of energy levels, because in this way we can trace the change of each level in Fig. 3. We see that in the very narrow interval of pressure below 8.85 kbar, the $2s$ and $3s$ levels rapidly fall down and the pairs of levels $(1s,2s)$ and $(2s,3s)$ become very close to each other. At higher pressures, the $3s$ and $2s$ levels replace the $2s$ and $1s$ levels, respectively, and the $1s$ (ground-state) energy level very steeply decreases becoming a deep level at very high pressure. The parameter $\gamma = -0.168$ eV has been adjusted in order to obtain the correct position of the anticrossing on the pressure scale. The quantitative agreement between the calculated and measured[5] positions of levels that are on the energy scale is obtained without any fitting.

The energy levels that are connected with the donor states of different localization approach each other under influence of the external perturbation (in this case, the hydrostatic pressure). These donor states possess the same (*s*) symmetry; therefore, they repel each other (in a sense of the perturbation theory). The resulting anticrossing is very sharp and occur in the very narrow interval of pressure, which gives evidence of the very weak level repulsion. The minimum separation between the $1s$ and $2s$ energy levels is calculated to be 0.1 meV, while this value fitted by Wasilewski and Stradling[5] is 0.5 meV. Our calculations show that the similar anticrossings as well appear for higher energy levels of *s* symmetry.

The anomalous anticrossing results from the electron-LA-phonon coupling.[21] This effect appears for the donor states of the different localization, which are accompanied by the different lattice deformation. In comparison with the ionized donor, the crystal lattice is strongly modified for the highly localized donor state, while the lattice remains almost unchanged for the donor states of the weak localization. Under influence of the hydrostatic pressure, the energy levels that are associated with both the types of donor states become very close before they begin to repel each other. ''The strength'' of this level repulsion is determined by the value of overlap (20) between the corresponding phonon states, which considerably differ between themselves if the lattice distortion is so different. This yields the very small value of overlap (20), which takes on the value of about 10^{-3} for 9 kbar. This in turn leads to the very weak level repulsion, which is responsible for the extremely sharp anticrossing.

The level anticrossing can be observed if some external perturbation changes the relative position of the energy levels. Besides the external pressure, the external magnetic field can also cause this effect.[2] Therefore, we expect that the similar properties of donor states can be found as a function of the magnetic field. The hydrostatic pressure considered in this work changes the electron-band mass, static dielectric constant, and width of the conduction band. The changes of the band mass and the dielectric constant affect the weakly localized donor states, which leads to a slight change of the hydrogenlike spectrum. The change of the conduction-band width is more important in the description of anticrossing because it shifts the energy levels of both the types of donor states into the same energy range.

The present approach as well includes the coupling with LO phonons, which has no influence on the anomalous anticrossing (cf. dotted curves in Fig. 3). However, the Fröhlich coupling considerably changes the donor properties in the ionic CdF_2 crystal[35] and, even in the weakly ionic GaAs crystal, possesses the remarkable influence on the shallow-level donor states of weak localization. The results displayed in Fig. 3 show that taking into account this coupling leads to the 15% shift of the $1s$ energy level as compared with that obtained without LO phonons, which would be located at $E = -R_D$ (donor Rydberg with static dielectric constant).

In Sec. II, we discussed the way of choosing the phenomenological parameters used in the calculations. Since not all these parameters can be uniquely determined from experimental data, we now discuss possible effects of uncertainties in this choice.

First, we comment on the assumption made for the conduction-band shape [Eq. (24)]. We have checked that the results of the calculations do not change if we use another

form of dispersion relation provided that $E^c_{\mathbf{k}}$ fulfills the same boundary conditions for small and large $|\mathbf{k}|$. The correct reproduction of the conduction band in the nearest neighborhood of the Γ point is important for the weakly localized states, while the average conduction band determines the strongly localized donor states.

The results can be sensitive to the uncertainty in the pressure coefficient $d\Delta/dp$. However, we have checked that the 5% change of this coefficient in the interval 8.85 kbar $\leqslant p \leqslant 9.15$ kbar, in which the experimental points corresponding to the highly localized states of the lowest energy are located, leads to the shift of energy, which does not exceed 0.15 meV, i.e., 0.03 R_D. This change would not be visible in Fig. 3.

The present theoretical model consists of one fitting parameter γ, which determines the short-range potential of the impurity. In some materials, e.g., the Si crystal,[37] the values of γ for various donor species can be found from the measured chemical shifts if we introduce the so-called ''central-cell corrections.'' However, the chemical shifts for donors also possess other sources.[38,39] In our previous papers[40,41] on donors in GaAs, we analyzed the two mechanisms, which are caused by (i) short-range potential, which results from the difference in atomic cores between the host-crystal and impurity atoms (typical ''central-cell potential''), and (ii) long-range potential, which results from the redistribution of the valence electrons around the impurity center. The chemical shifts resulting from effect (ii) were described in our papers[40,41] with the help of the reorthogonalisation-charge model. This long-range potential can be approximated by the Coulomb potential.[40,41] For the donors of the strong electron localization, mechanism (i) is dominating, while for the very weakly localized donor states, like these in GaAs, it is mechanism (ii). Therefore, in GaAs, due to the very small electron mass and large donor Bohr radius, information obtained from the chemical shifts for the weakly localized donor states is less useful for the strongly localized donors and vice versa. The interpretation of the chemical shifts for the donors of weak localization in GaAs as resulting exclusively from the central-cell potential yields the short-range potential wells, which are too deep.[42,43] The central-cell potential obtained in Ref. 42 can bind the electron in the highly localized state of the energy lower than the energies of the core states, which is an unphysical result. On the contrary, the short-range potential for Ge donor in GaAs fitted by us in order to get the correct value of pressure for the anticrossing ($\gamma = -0.168$ eV) leads to the negligibly small (0.002 meV) central-cell correction for the weakly localized donor.

Because of these problems with receiving the reasonable values of the central-cell corrections for donors in GaAs, we have to treat γ as the adjustable parameter. Its value is taken on from the measured value of pressure, at which the anticrossing appears for the Ge impurity. We have found that the anticrossing pressure is a nearly linear function of the parameter γ, i.e., the increase of γ by 0.1 eV leads to the growth of this critical pressure by about 10 kbar. Nevertheless, we should realize that this parameter is connected with the energy of the strongly localized donor state. Therefore, when fitting γ we compensate an eventual error in the parameter Δ [Eq. (24)]. The change of Δ affects the average kinetic energy of the localized electron, which gives rise to the corresponding change of the average potential energy, i.e., parameter γ. We have estimated that the increase of Δ by 0.1 eV brings about the decrease of γ by 0.095 eV. The simultaneous change of both the parameters in such a way that the value of the anticrossing pressure is fixed does not change the properties of the considered donor states.

The results shown in Fig. 4 provide an indirect proof of a possibility of using the one-element basis for the donor states of different localization, which is assumed in the Toyozawa model[31] of donor metastability. We see from Fig. 4 that, with an exception of the narrow region of anticrossing, the donor states are either weakly or strongly localized. Therefore, each of them can be approximately described by the one function of either weak or strong localization.

The anticrossing is closely connected with the metastability of the donor states.[33] The estimated phonon part [Eq. (40)] of the transition probability allows us to discuss this effect (Fig. 5). The total transition probability is dominated by the phonon contribution, which changes it by many orders of magnitude. Thus, in this discussion, we neglect the electronic contribution [Eq. (35)], since taking into account its actual value would not change our conclusions. We have calculated the lower and upper bounds on the phonon factor of the transition probability for the donors in the two materials: GaAs and CdF_2. Having calculated the upper bound, we can answer the question if does the metastability occur, i.e., the transition probability is certainly less than this upper bound. On the other hand, the calculated lower bound permits us to trace the disappearance of the metastability. In Fig. 5, we see that the probability of radiative transitions from the excited state increases (at least as quickly as its lower bound) with the increasing separation between the energy levels. As a result, the life time of the excited state becomes small and the metastability vanishes.

One can observe the considerable reduction of the transition probability for CdF_2, which results from the strong electron-phonon coupling. This result allows us to explain the observed[3,4] metastability of the weakly localized excited states of single donors. Moreover, in CdF_2, the one-electron donor states of the weak and strong localization can coexist, which as well is in agreement with experiment.[3,4] The two upper curves in Fig. 5 correspond to GaAs, for which we do not expect any metastability for the one-electron donor states. However, the metastability is not excluded for the two-electron donor states (of D^- or *DX* type). This suggestion can be supported by the following argumentation: For the two-electron states, we have to include the phonon interaction amplitude for each electron (i.e., twice) in the argument of exponential function in overlap (20), which is the multiplication factor in expression (40) for the transition probability. This gives us the factor 4 in the exponent [Eq. (20)] and, as a consequence, the transition probability for the two-electron donor state can be estimated as the fourth power of that value for the one-electron donor state. This reduces the transition probability by many orders of magnitude. We expect that taking into account the electron-electron interaction will enhance this effect. Therefore, the present mechanism of the metastability is not excluded for the two-electron donor centers in GaAs.

This mechanism provides an alternative explanation of the nature of *DX* center in GaAs. Its essence is in agreement

with the Chadi-Chang model,[10] since both the models take into account the large lattice distortion and two-electron occupancy of the donor states. In our approach, the lattice distortion is described with the help of phonons. On the contrary to Toyozawa[31] who assumes the continuum model of lattice deformation, the present work is based on the discrete description of the crystal lattice vibrations.

V. CONCLUSIONS

We have proposed a unified theory for the neutral donor states of different localization. The present treatment is based on the one-band approximation for the electron states and discrete description of the lattice vibrations. This approach provides a realistic picture for the strongly localized donor states and goes over into the effective-mass approximation for the weakly localized donor states. We have shown that the states of the weak and strong localization can coexist on the same donor impurity. If the strongly localized state is the ground state of the system, there exist the excited states, which possess the weak localization and shallow (hydrogenlike) energy levels. The spectrum of these weakly localized states is nearly identical, if the strongly localized state is resonant with the conduction band. The donor states of both the types exhibit very interesting properties if their energy levels lie close to each other. Then, the extremely sharp and narrow anticrossing appears between the energy levels connected with the states of the same symmetry. The results of the present paper for GaAs under high hydrostatic pressure allow us to explain the nature of the anomalous anticrossing between the donor energy levels observed in this material. This effect results from the different lattice deformations around the impurity center for the donor states of different localization. The main contribution to the lattice deformation in GaAs results from the short-range electron-LA phonon coupling.

We have shown that there exists the close relationship between the anticrossing and metastability of donor states. The metastability is also caused by the difference in the lattice deformation around the impurity center for the donor states of different localization and appears if the separation of the energy levels belonging to the weakly and strongly localized donor states is small enough. We have estimated the phonon part of the transition probability from below and from above which permits us to draw the conclusions on the appearance and disappearance of the metastable occupancy of the donor states. We have shown that the metastability disappears if the energy level of the strongly localized state is located too low, i.e., the energy separation between this level and the shallow levels becomes considerably larger than the LO phonon energy.

The eigenvalue problem for the electron-donor-phonon system has been solved by the variational means in the wave-vector space. We have developed the method, which allows us to obtain the excited states being correctly orthogonalized to all the states of lower energy, including the many-phonon states. These many-phonon states have been also taken into account in the present estimates of the transition probability.

ACKNOWLEDGMENTS

We are grateful to Professor J. M. Langer and Professor J. T. Devreese for stimulating discussions. This work has been partially supported by the Commission of the European Communities under Contract No. ERBCIPDCT94-0032.

APPENDIX

The phonon factor [Eq. (40)] of the transition probability includes the contributions of both the LO and LA phonons. If we consider the contribution of the LO phonons only, the value of expression (40) can be evaluated analytically, which cannot be done for LA phonons. In the Appendix, we present the method of calculation of the lower and upper bounds on the transition probability (40). We confine ourselves to the LA phonons and omit the index σ of the phonon branch. We introduce the following notation:

$$x_{\mathbf{q}}=|g_{1\mathbf{q}}-g_{0\mathbf{q}}|^2, \tag{A1}$$

and

$$X=\sum_{\mathbf{q}} x_{\mathbf{q}}. \tag{A2}$$

Equation (40) can be written in the explicit form

$$P_{ph}=(\Delta E)^{-1}e^{-X}\sum_{N=0}^{\infty}\frac{1}{N!}\sum_{\mathbf{q}_1\cdots\mathbf{q}_N}\prod_{j=1}^{N}x_{\mathbf{q}_j}\Delta E_N\Theta(\Delta E_N). \tag{A3}$$

In Sec. II, we have assumed that all the phonon quantities are isotropic, i.e., they depend on the wave-vector length $q=|\mathbf{q}|$ only. So, in the Appendix, we use the q-dependent quantities: $\omega(q)$, $x(q)$, etc. Therefore, the N-fold summation over the Brillouin zone can be performed in order of the decreasing wave-vector length, which for the LA phonons corresponds to the decreasing phonon energy. This means the following replacement in Eq. (A3):

$$\frac{1}{N!}\sum_{\mathbf{q}_1\cdots\mathbf{q}_N}\rightarrow\sum_{q_1>\cdots>q_N}. \tag{A4}$$

Simultaneously, each summation over the Brillouin zone in Eq. (A3) is replaced by the integration over the Debye sphere of the radius Q and the angle integration is performed, i.e.,

$$\sum_{\mathbf{q}}\cdots\rightarrow\frac{\Omega}{2\pi^2}\int_0^Q dq q^2\cdots. \tag{A5}$$

In Eq. (A3), N is the number of LA phonons with total energy belonging to the interval (E_0,E_1). Therefore, N can take on arbitrary large values, which makes it impossible to perform the N-fold summation over $\mathbf{q}$ (integration over q). In order to overcome this problem, we divide each Debye sphere into $\mathcal{M}$ subintervals with the endpoints: $q_\mu=\mu(Q/\mathcal{M})$, where $\mu=1,\ldots,\mathcal{M}$. Employing the monotonicity of the LA phonon energy as a function of q, we can substitute into Eq. (A3) the corresponding values taken at the upper or lower endpoints of these subintervals, which leads to lower or upper bounds on P_{ph}, respectively. If we take on the phonon energies corresponding to the upper limits of the subintervals, we obtain the lower bound

$$\Delta E_N^L = \Delta E - \sum_{j=1}^{N} \hbar\omega(q_{\mu_j}) \leqslant \Delta E_N , \tag{A6}$$

which is a piecewise constant function of q. For each j, we integrate over $\mathcal{M}$ subintervals of q and introduce

$$Y_\mu = \frac{\Omega}{2\pi^2} \int_{q_{\mu-1}}^{q_\mu} dq q^2 x(q). \tag{A7}$$

This provides us with the following lower bound on the probability P_{ph}:

$$P_L = (\Delta E)^{-1} e^{-X} \sum_{N=0}^{\mathcal{N}} \sum_{\mu_1 > \cdots > \mu_N} \prod_{j=1}^{N} Y_{\mu_j} \Delta E_N^L \Theta(\Delta E_N^L). \tag{A8}$$

In Eq. (A8), the sum over μ_1 runs from 1 to $\mathcal{M}$ and the sums over the other indices μ_j run from 1 to μ_{j-1}. Since all the terms of the sums in Eq. (A8) are positive, we can truncate the summation for every finite $\mathcal{N}$. Therefore, for finite $\mathcal{N}$ and $\mathcal{M}$, the following inequality is fulfilled:

$$P_L \leqslant P_{ph} . \tag{A9}$$

If $\mathcal{N} \to \infty$ and $\mathcal{M} \to \infty$, then $P_L \to P_{ph}$.

In order to obtain the upper bound on P_{ph}, we proceed in a similar way. However, we have to increase the terms in the right-hand side of Eq. (A3). Now, we cannot truncate the infinite series; therefore, we separate out the finite number of terms leaving the rest. The infinite sum over these rest terms can be performed, which gives the exponential function. As a result, we get the upper bound $P_U \geqslant P_{ph}$ of the following form:

$$P_U = (\Delta E)^{-1} e^{-X} \left[\sum_{N=0}^{\mathcal{N}} \sum_{\mu_1 > \cdots > \mu_N} \prod_{j=1}^{N} Y_{\mu_j} \Delta E_N^U \Theta(\Delta E_N^U) + \sum_{\mu_1 > \cdots > \mu_{\mathcal{N}}} \prod_{j=1}^{\mathcal{N}} Y_{\mu_j} e^{Z_n} \Delta E_{\mathcal{N}}^U \Theta(\Delta E_{\mathcal{N}}^U) \right], \tag{A10}$$

where

$$\Delta E_N^U = \Delta E - \sum_{j=1}^{N} \hbar\omega(q_{\mu_j - 1}) \geqslant \Delta E_N , \tag{A11}$$

and

$$Z_n = \sum_{j=1}^{n} Y_{\mu_j}, \tag{A12}$$

with n being determined by the two inequalities: $n \leqslant \mu_{\mathcal{N}+1}$ and $\hbar\omega(q_n) \leqslant \Delta E_{\mathcal{N}+1}^U$. The first term in Eq. (A10) has the form similar to that of the lower bound P_L [cf. Eq. (A8)]; the only difference is in the energetic argument. If the number $\mathcal{M}$ of divisions of the Debye sphere into the integration intervals increases, both these terms, i.e., P_L and the first term in the right-hand side of Eq. (A10) approach each other. For sufficiently large $\mathcal{N}$, the second term in Eq. (A10) can be reduced to a very small value. In the present calculations, we have obtained the closely lying lower and upper bounds on P_{ph} for $\mathcal{N} \simeq 10$ and $\mathcal{M} \simeq 12$.

[1] S. Porowski, M. Kończykowski, and J. Chroboczek, Phys. Status Solidi A **63**, 291 (1974).
[2] Z. Wasilewski, A.M. Davidson, R.A. Stradling, and S. Porowski, Physica **117B-118B**, 89 (1983).
[3] U. Piekara, J.M. Langer, and B. Krukowska-Fulde, Solid State Commun. **23**, 583 (1977).
[4] J.E. Dmochowski, J.M. Langer, Z. Kaliński, and W. Jantsch, Phys. Rev. Lett. **56**, 1735 (1986).
[5] Z. Wasilewski and R.A. Stradling, Semicond. Sci. Technol. **1**, 264 (1986).
[6] J.E. Dmochowski, Z. Wasilewski, and R.A. Stradling, Mater. Sci. Forum **65-66**, 449 (1990).
[7] J.E. Dmochowski, R.A. Stradling, P.D. Wang, S.N. Holmes, M. Li, B.D. McCombe, and W. Weinstein, Semicond. Sci. Technol. **6**, 476 (1991).
[8] J.E. Dmochowski and R.A. Stradling, Jpn. J. Appl. Phys. **32**, Suppl. 32-1, 227 (1993).
[9] P.J. van der Wel, P. Wisniewski, T. Suski, J. Singleton, C. Skierbiszewski, L.J. Giling, R. Warburton, P.J. Walker, N.J. Mason, R.J. Nicholas, and M. Eremets, J. Phys. Condens. Matter **5**, 5001 (1993).
[10] D.J. Chadi and K.J. Chang, Phys. Rev. Lett. **61**, 873 (1988).
[11] J. Dąbrowski and M. Scheffler, Mater. Sci. Forum **83-87**, 735 (1992).
[12] T. Fujisawa, J. Yoshino, and H. Kukimoto, Jpn. J. Appl. Phys. **29**, L388 (1990).
[13] P. Gibert, D.L. Williamson, J. Moser, and P. Basmaji, Phys. Rev. Lett. **65**, 1144 (1990).
[14] T.N. Theis, P.M. Mooney, and B.D. Parker, J. Electron. Mater. **20**, 35 (1990).
[15] L. Dobaczewski and P. Kaczor, Phys. Rev. B **44**, 8621 (1991).
[16] M. Baj, L.H. Dmowski, and T. Słupiński, Phys. Rev. Lett. **71**, 3529 (1993).
[17] S. Bednarek and J. Adamowski, Mater. Sci. Forum **65-66** 427 (1990).
[18] S. Bednarek and J. Adamowski, Mater. Sci. Forum **83-87** 493 (1992).
[19] Y. Cai and K.S. Song, J. Phys. Condens. Matter **7**, 2275 (1995).
[20] S. Bednarek and J. Adamowski, in *The Physics of Semiconductors*, edited by D.J. Lockwood (World Scientific, Singapore, 1995), p. 2335.
[21] S. Bednarek and J. Adamowski, Phys. Rev. B **51**, 4687 (1995).
[22] E. Yamaguchi, K. Shiraishi, and T. Ohno, J. Phys. Soc. Jpn. **60**, 3093 (1991).
[23] W. Trzeciakowski and J. Krupski, Solid State Commun. **44**, 1491 (1982).
[24] A. Neethiulagarajan and S. Balasubramanian, Phys. Rev. B **48**, 9114 (1993).
[25] U. Ekenberg, Phys. Rev. B **36**, 6152 (1987).
[26] T. Ruf and M. Cardona, Phys. Rev. B **41**, 10 747 (1990).
[27] J.M. Shi, F.M. Peeters, and J.T. Devreese, Phys. Rev. B **48**, 5202 (1993).

[28] Ya.B. Zel'dovich, Fiz. Tverd. Tela **1**, 1637 (1959) [Sov. Phys. Solid State **1**, 1497 (1960)].
[29] L. Resca, Phys. Rev. B **26**, 3238 (1982).
[30] W. Pötz and P. Vogl, Solid State Commun. **48**, 249 (1983).
[31] Y. Toyozawa, Physica **116B**, 7 (1983).
[32] S. Bednarek and J. Adamowski, Acta Phys. Pol. **84**, 820 (1993).
[33] S. Bednarek and J. Adamowski, Solid State Commun. **91**, 429 (1994).
[34] P.M. Platzman, Phys. Rev. **125**, 1961 (1962).
[35] J. Adamowski, Phys. Rev. B **32**, 2588 (1985).
[36] P.-O. Löwdin, Phys. Rev. **139**, A357 (1965).
[37] L.E. Oliveira and L.M. Falicov, Phys. Rev. B **33**, 8765 (1986).
[38] S.T. Pantelides, Rev. Mod. Phys. **50**, 797 (1978).
[39] M. Lannoo and J. Bourgoin, *Point Defects in Semiconductors* (Springer-Verlag, Berlin, 1981), Vol. I.
[40] S. Bednarek and J. Adamowski, in *Shallow Impurities in Semiconductors 1988*, Institute of Physics Conference Series Vol. 95, edited by B. Monemar (Institute of Physics, Bristol, 1988), p. 539.
[41] S. Bednarek, in *Proceedings of the 19th International Conference on the Physics of Semiconductors*, edited by W. Zawadzki (Institute of Physics, Polish Academy of Sciences, Warsaw, 1988), p. 1277.
[42] D. Chandramohan, S. Balasubramanian, and M. Tomak, Phys. Rev. B **37**, 7102 (1988).
[43] The magneto-optical studies [H. R. Fetterman *et al.*, Phys. Rev. Lett. **26**, 975 (1971); J. H. M. Stoelinga *et al.*, J. Phys. Chem. Solids **39**, 873 (1978)] show that the relative chemical shifts for shallow-level donors in GaAs are proportional to the square of the donor-envelope wave function at the center. The absolute values of the central-cell potential well deduced from these data are still too large.